



Research article

UAV search coverage under priority of important targets based on multi-location domain decomposition

Xiaoying Zheng¹, Jing Wu^{2,*}, Xiaofeng Li^{3,*}, Junjie Huang²

¹ School of Mathematics and Science, Wuhan Institute of Technology, Wuhan 430073, China

² Department of Operations and Planning, Naval University of Engineering, Wuhan 430030, China

³ College of Power Engineering, Naval University of Engineering, Wuhan 430030, China

* **Correspondence:** Email: wj82116@126.com, xiaofengli@whu.edu.cn.

Abstract: In recent years, the coverage path planning (CPP) of unmanned aerial vehicles (UAVs) has attracted attention in reconnaissance, patrol, and search and rescue efforts, aiming to plan the paths for UAVs to cover a specified area as efficiently as possible. This paper proposes a UAV path fast coverage model to prioritize important targets with domain composition based on the starting point and location of the targets, combined with the domain decomposition strategy of important targets. Considering the constraints of the number of UAVs, the number of operators, and the flight time, the parallel search strategy can plan the coverage scheme with the shortest search time for the search range, and further obtain the coordinate points and path coordinates of the UAV turning. Finally, through multiple simulation experiments in four maps of various islands, the proposed method is verified to have an improved performance compare to the two track path coverage algorithms methods in terms of the coverage efficiency and the time complexity, thus providing a more scientific basis for the path coverage research of multi-target searches.

Keywords: mathematical model; multitasking; path planning; search methods; process planning

1. Introduction

In recent years, the continuous application of UAVs in agriculture, military, transportation, and other fields has sparked growing interest in understanding search areas and coverage methods. UAV CPP is a technique that enables the planning of paths for UAVs to cover a specified area as efficiently

as possible. The primary objective of UAV CPP is to ensure the complete coverage of the area by the UAV while minimizing the time and distance traveled [1]. Notably, the identification of important targets and the constraints of a priority search have assumed an increasingly crucial role in UAV reconnaissance, patrol operations, and urban searches [2,3].

UAV path planning refers to the process of designing a flight path for the UAV to fly from the starting point to the target point [4,5]. The primary goal of path planning is to identify the most efficient and safe flight path for the UAV. The UAV path coverage refers to the process of ensuring that the UAV flies over the entire area of interest while avoiding obstacles, thus ensuring safety. The main distinction between path planning and the path coverage is that path planning only requires finding the most efficient and safe path from the starting point to the target point, while the path coverage necessitates ensuring the complete coverage of the entire area of interest. Furthermore, path planning typically only considers the location of obstacles, while the path coverage also needs to take the shape and size of the area of interest into account [6,7]. The identification and search for important targets can enhance the overall search efficiency, refine the regional coverage strategy, and facilitate other practical tasks. It is dictated by specific issues and experiences, such as densely populated areas in search and rescue operations and command posts in military operations [8–10]. The presence of multiple targets with different priorities has increased the complexity of the area coverage search, multi-UAV target allocation, and path planning. With the progression of research, numerous researchers have proposed numerous effective algorithms for the problem of UAV trajectory path coverage, ranging from the initial few traditional algorithms to the currently prevalent swarm intelligence optimization algorithms [11–14]. Popular UAV trajectory path coverage algorithms may encompass the following approaches: ant colony optimization (ACO), artificial potential field (APF), particle swarm optimization (PSO), the genetic algorithm (GA), and the artificial bee colony algorithm (ABC) [15–18]. These methods have achieved some progress in enhancing the efficiency of path planning in practical applications [19–21].

On the contrary, there is a paucity of research on the path coverage in the context of the priority search for important targets, and the time complexity and coverage efficiency of some proposed methods require further enhancements [22,23] when the search for islands and reefs with substantial resources holds immense military significance. This paper presents a path coverage model with a priority search for important targets based on the association between targets and the search area in conjunction with the search strategy. A novel search coverage strategy for islands and reefs can be devised by identifying the priority of important targets and integrating it with the optimization model for the area coverage. The application and comparison of island and reef coverage can be demonstrated under the new area search model and other methods with a UAV target priority. By comparing two prevalent UAV trajectory path coverage algorithms, the rationality and effectiveness of the method with varying numbers of UAVs are evaluated via multiple UAV reconnaissance simulation experiments in four maps of island and reef areas.

2. Materials and methods

Based on the differences in reconnaissance objects, multi-UAV cooperative area coverage can be divided into two categories: “point-to-point” cooperative search and “point-to-face” cooperative search [14,24]. The “point-to-point” cooperative search focuses on specific target points and is suitable for search tasks that require the optimization of specific target points, which can effectively improve

the search efficiency and accuracy. On the other hand, the “point-to-face” cooperative search, can be suitable for searching large mission areas and is applicable to search tasks that require covering large areas or finding unknown targets. The “point-to-face” cooperative search method is more difficult than the “point-to-point” method, though it is suitable for searching in partially unknown environments, this enabling a full search of the area at a minimal cost.

2.1. Optimal coverage direction & search line spacing under parallel search

In the reconnaissance search task, the search strategy based on a parallel line is usually selected for the constraint of the UAV performance. In order to obtain the optimal covering direction of a given polygon region, some researchers can use the search direction under the minimum height strategy [14,25], that is, the searched polygon region can be rotated to the direction of the plane corresponding to the minimum height (h_{\min}). Suppose the width of the image sensor can be represented by a , the focal length of the device can be represented by b , and the flight height (i.e., the distance between the device and the ground) can be represented by H . Combined with the principle of triangle similarity, the width of the device footprint L can be calculated by the following formula and is cited (1):

$$L = H \frac{a}{b}. \quad (1)$$

Let the proportion of overlap be $c \in (0,1)$, and the search interval d_l can be cited (2) as follows:

$$d_l = \frac{h_{\min}}{N_l}, N_l = \left\lceil \frac{h_{\min}}{L(1-c)} \right\rceil, \quad (2)$$

where N_l denotes the number of covered rows, and $\lceil \cdot \rceil$ denotes the upward rounding, which can be determined by the minimum height and flight height with non-overlap ratio. As shown in Figure 1, for a covered rectangular area (black line), the graph $G = (V, E)$ can be used to represent the set of key nodes in the search process and the set of edges formed by the order. The starting point is the coordinate of the UAV launch position (blue) and the two boundary points related to the search path in the first line. Based on the coordinates of the search area entered, the search coverage area is identified, and the optimal coverage direction is determined using the minimum height strategy as parallel to the x-axis; the coverage row spacing is determined using the strategy based on similar triangles. The intersection of the coverage flight path and the regional boundary is used as the extreme point (between the path under the parallel search strategy and the boundary of the region) of the coverage row (red).

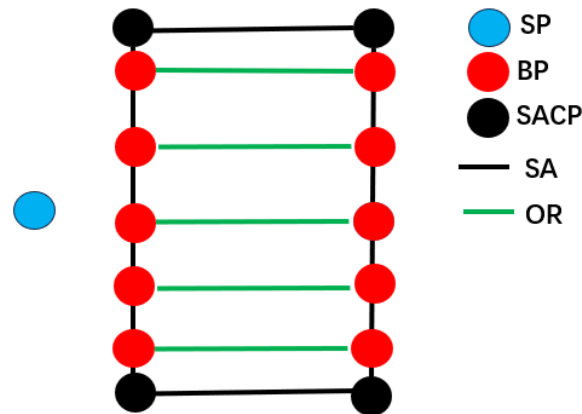


Figure 1. Example diagram of domain decomposition (The abbreviations are described in Appendix A).

2.2. Multi-UAV search coverage model in single region

Suppose the single area G can be represented by an $N \times N$ distance matrix C , $C_{ij} = \text{dis}(i, j)$, where dis is denoted by the Euclidean distance, $V_{ij}^k \in \mathbb{R}$ can represent the flight speed of the k -th UAV from vertex i to vertex j , the constant $t_s \in \mathbb{R}$ can represent the setup time of the UAV, m can be used to represent the number of UAVs, $O \in \mathbb{N}$ is the number of UAV operators, and $N \in \mathbb{N}$ is the number of nodes of the graph. Finally, the variable d_k can represent the rest of the time required to launch the k -th UAV. Let X_{ij}^k be the decision variable of the model as follows:

$$X_{ij}^k = \begin{cases} 1 & \text{The } k\text{-th UAV flies from vertex } i \text{ to vertex } j, \\ 0 & \text{The } k\text{-th UAV does not from vertex } i \text{ to vertex } j. \end{cases}$$

Let T_k is the total time required for coverage; then, the objective function can be taken by the k -th UAV to fly the corresponding route [14] and is cited (3) as follows:

$$\begin{aligned} T_k &= \sum_{i=1}^N \sum_{j=1}^N \frac{C_{ij}}{V_{ij}^k} X_{ij}^k + d_k, \\ d_k &= t_s \left\lceil \frac{k}{O} \right\rceil \sum_{j=1}^N X_{1j}^k, k = 1, \dots, M. \end{aligned} \quad (3)$$

In a task where only one operator operates the whole UAV team, and k -th UAV will have the additional time d_k . When the UAV is in an idle state, d_k will be zero. If X_{1j}^k is zero, O can denote the number, thus indicating that the k -th UAV has not left node 1 to represent the launch position. Considering the constraints of the UAVs node search, the number and running time, the single-region coverage model includes the following constraints: each node of the graph can be required to be visited only once by one UAV (cited (4), cited (5)); the subtour elimination constraint can ensure that the search path has no internal loops and be cited (6); the UAVs can cover the area modeled by graph G and be cited (7); and allow the number m of the UAVs can be used in the mission to be smaller than

the maximum number m of available UAVs (cited (8) and (9)). The planning model of the multi-UAV search coverage path in a single area G can be obtained as follows:

$$T(G) = \text{Max}(T_k) = \sum_{i=1}^N \sum_{j=1}^N \frac{C_{ij}}{V_{ij}^k} X_{ij}^k + t_s \left[\frac{k}{O} \right] \sum_{j=1}^N X_{1j}^k, k = 1, 2, \dots, M.$$

$$\left. \begin{array}{l} \sum_{k=1}^M \sum_{i=1}^N X_{ij}^k = 1, j = 2, 3, \dots, N, \\ \sum_{i=1}^N X_{ip}^k - \sum_{j=1}^N X_{pj}^k = 0, p = 1, 2, \dots, N, k = 1, 2, \dots, M, \\ u_i - u_j + N \sum_{k=1}^M X_{ij}^k \leq N - 1, u_i \in \mathbb{Z}, i, j = 2, 3, \dots, N, \\ \sum_{k=1}^M X_{i,i+1}^k + \sum_{k=1}^M X_{i+1,i}^k = 1, i = 2, 4, \dots, N, \\ \sum_{k=1}^M \sum_{j=1}^N X_{1j}^k = m, \\ m \leq M. \end{array} \right\} \text{s.t.} \quad \begin{array}{l} (4) \\ (5) \\ (6) \\ (7) \\ (8) \\ (9) \end{array}$$

2.3. Multi-targets-first UAV search coverage model

Considering the situation that there are several important targets with known positions in the search area, the search strategy can be related to the starting point of the UAV, the region of decomposition, and the location relationship between the search boundary points and the important targets [26,27]. According to the actual needs, there are usually no more than three important targets in an area searched by one UAV. If more than three targets are searched, the search coverage can be carried out by either clustering or adding UAVs [28,29]. As shown in Figure 2, the area occupied by the target is negligible compared to that of the region under the condition of being as uniform as possible, and count the targets included in the divided region. For the region G containing a single target O_1 , set r UAV turning points as (n_1, n_2, \dots, n_r) .

Based on the constraint condition of the priority search, find the closest turning point, $n_0 = \min_i \text{dis}(n_i, O_1)$ (node 6) to the target, and its corresponding side turning point is (node 5), the upper and lower turning points, $n_A^{G_1} \in G_1, n_A^{G_2} \in G_2$, (nodes 4 and 8), and the search row, $n_0 \rightarrow n_0'$, naturally divides G into G_1 and G_2 . According to the setting of the turning point, it is easy to obtain the boundary turning points, $n_B^{G_1}, n_B^{G_2}$, (nodes 1 and 9) of G_1 and G_2 , respectively. At this time, the modeling of the priority path coverage of multiple UAVs is transformed into the problem of allocating the turning points under a uniform division. After determining the turning point after the priority search of the target row, the total search coverage time T_{sz} can be determined. The total time T_{sz} of the search coverage model with single target priority includes three parts: the search time of two area, the time row where the target is located, and the shortest path search time between the boundaries of G_1 and G_2 , which can be expressed by the following formula:

$$T_{sz} = T_{n_0 \rightarrow n_0} + T(G_1) + T(G_2) + \min\left(T_{n_A^{G_1} \rightarrow n_B^{G_2}}, T_{n_A^{G_2} \rightarrow n_B^{G_1}}\right), \quad (10)$$

where $T_{n_0 \rightarrow n_0}$ is the search time for flying along the search row, and $T_{n_A^{G_1} \rightarrow n_B^{G_2}}$ and $T_{n_A^{G_2} \rightarrow n_B^{G_1}}$ are the time from the turning point $n_A^{G_1}$ to the boundary turning point $n_B^{G_2}$ and the turning point $n_A^{G_2}$ to the boundary turning point $n_B^{G_1}$, respectively, which are related to the path length. The $T(G_1), T(G_2)$ is performed starting from the turning points, $T(G_1), T(G_2)$, respectively; then, the coverage (in the target-free area) is calculated (see Section 2.2).

Suppose the area is evenly divided according to the number of drones. Taking the path coverage of the area G containing multiple targets, O_1, \dots, O_v , as an example, $1, \dots, v$ represents the priority of the target, and the UAV turning points corresponding to v targets are set as (n_1, n_2, \dots, n_v) .

Based on the constraint condition of the target priority search, find the search rows, $(n_1 \rightarrow n_1, n_2 \rightarrow n_2, \dots, n_v \rightarrow n_v)$, where the closest turning points corresponding to the v targets are located, and divide the area into $v + 1$ parts, which are denoted as $(G_1, \dots, G_v, G_{v+1})$. The search row corresponding to the v -th priority target is $n_r \rightarrow n_r$, and this search row can divide the area into $G_q = G_1 \cup G_2 \cup \dots \cup G_v$ and G_{v+1} . Combined with the parity of the UAV turning points, determine the starting turning node, $n_A^{G_q} \in G_q, n_A^{G_{v+1}} \in G_{v+1}$, and boundary turning point, $n_B^{G_q} \in G_q, n_B^{G_{v+1}} \in G_{v+1}$, corresponding to the upper and lower areas of node n_r . The total search coverage time T_{sz} can be determined by the turning point after the priority search of the target row, which can be calculated by the following formula:

$$T_{sz} = T_{n_1 \rightarrow n_1 \rightarrow n_2 \rightarrow n_2 \rightarrow \dots \rightarrow n_v \rightarrow n_v} + T(G_q) + T(G_{v+1}) + \min\left(T_{n_A^{G_q} \rightarrow n_B^{G_{v+1}}}, T_{n_A^{G_{v+1}} \rightarrow n_B^{G_q}}\right), \quad (11)$$

where $T_{n_1 \rightarrow n_1 \rightarrow n_2 \rightarrow n_2 \rightarrow \dots \rightarrow n_v \rightarrow n_v}$ is the time to ensure the priority search of v targets, $T_{n_A^{G_q} \rightarrow n_B^{G_{v+1}}}$, $T_{n_A^{G_{v+1}} \rightarrow n_B^{G_q}}$ are related to the paths from the turning point $n_A^{G_q}$ to the boundary turning point $n_B^{G_{v+1}}$ and the turning point $n_A^{G_{v+1}}$ to the boundary turning point $n_B^{G_q}$, respectively, and the search $T(G_q), T(G_{v+1})$ is performed starting from the turning points $n_A^{G_q} \in G_q, n_A^{G_{v+1}} \in G_{v+1}$, respectively; then, the coverage (in the target-free area) is calculated (see Section 2.2 for reference). As shown in Figure 2, the two turning rows corresponding to the two targets are node $3 \rightarrow 4$ and node $8 \rightarrow 7$, respectively. According to the search row, the corresponding upper and lower turning points are nodes 6 and 10, and the search row $7 \rightarrow 8$ naturally divides G into $G_1 \cup G_2$ and G_3 . According to the setting of the parity of the turning point, it is easy to obtain the boundary turning points of $G_1 \cup G_2$ and G_3 (nodes 1 and 13, respectively). In order to obtain the routes that each UAV must perform and the corresponding total minimum search one must minimize the time of the longest route among all UAV routes. By introducing the longest UAV route, the aforementioned optimization problem can be transformed into a linear problem to solve [14].

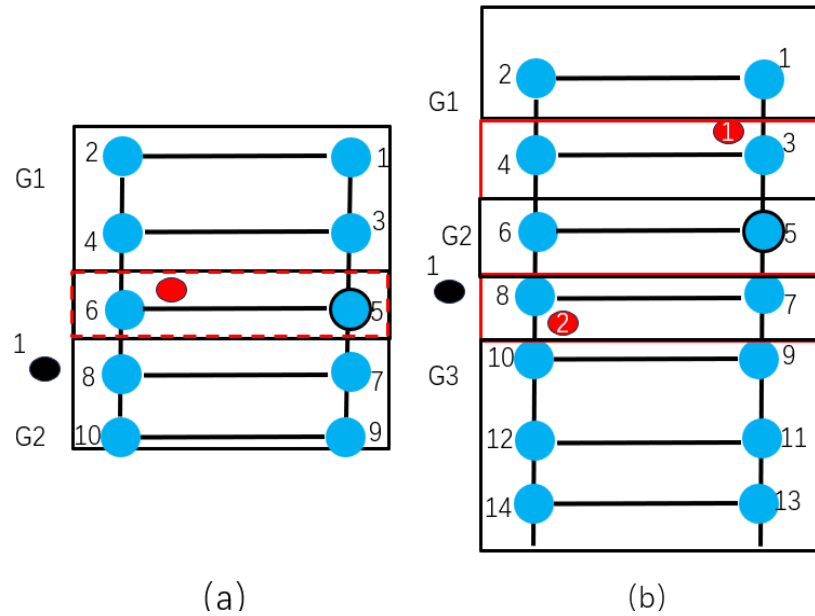


Figure 2. Schematic diagram of target priority search (The search of one target (left) and the search of two targets (right)).

2.4. Comparison of method

The search coverage efficiency is an important indicator to test the path search of UAVs [29]. Taking the coverage time T_0 proposed in the experiment as the benchmark, the total coverage time T_x of the comparative method in the same experiment is compared. The path search coverage efficiency (CE) with different numbers of UAVs is recorded using the following formula:

$$CE = \frac{T_x - T_0}{T_0}, \quad (12)$$

where a CE greater than 0 indicates that the proposed method has a higher search efficiency; on the contrary, it indicates that the proposed method has a lower coverage efficiency.

3. Results

In order to verify whether the model in Section 2 can effectively solve the task of multi-UAV reconnaissance on Jinghong Island and Hongxiu Island, the optimal coverage path scheme under multi-objectives can be given to set the unified rule. The UAV take-off needs to be set by an operator, and an operator cannot set multiple UAVs at the same time, though they can only operate in turn [30]. In order to uniformly compare the search process, the time to set 1 UAV can be 2 minutes.

3.1. Island and reef map preprocessing

The MATLAB software can be used to establish the x-y coordinate system on the map of Jinghong Island, as shown in Figure 3. The general search scope of the UAV can be determined by the coordinate points of the four search areas, mainly considering that the area can cover the known important targets

on the island. Important facilities, such as harbor pools and docks, have been artificially built under the island; therefore, they can also be included in the search coverage [31]. According to the domain decomposition strategy, the optimal search direction can be determined to be the minimum height perpendicular to the given area to minimize the number of turns of the UAV to save time cost; then, the boundary point of the UAV flight turning (blue) can be obtained. In reconnaissance and patrol tasks, the priority has been given to the possible firepower coverage, and the missile launcher can be determined as the priority search target.

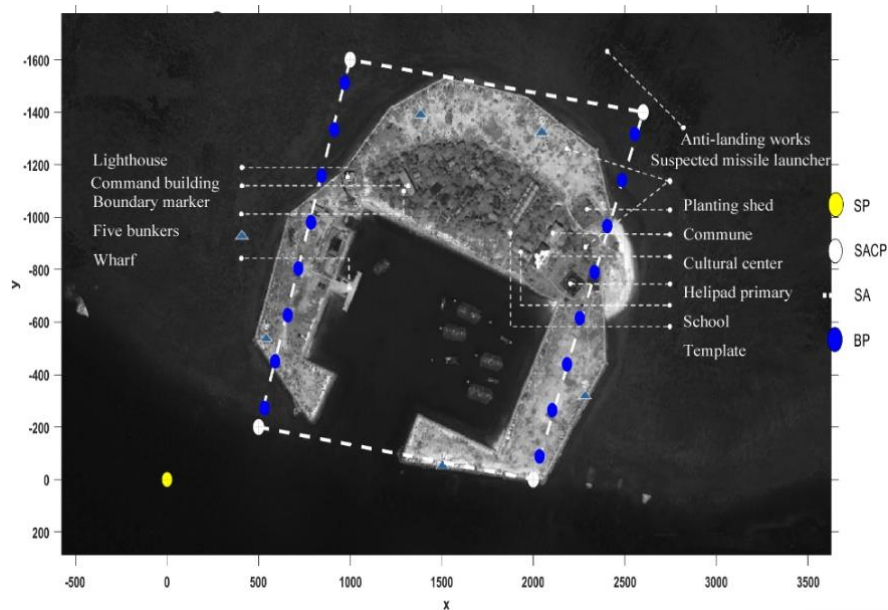


Figure 3. Search range map of Jinghong Island (The abbreviations are described in Appendix A).

On the map of Hongxiu Island in 2020, the command building is the organization and place for commanding the army to fight, which mainly enables commanders and command organs to carry out a stable and uninterrupted command of the army and play the role of the “brain”. The radar station is an important place for sea and air observation, and its main job is to find close ships, aircrafts, and other targets in time, thus playing the role of the “eyes”. Because of the small reflection area of the UAV, it is difficult to be detected. Therefore, we chose a command building and two radar stations in the figure as important targets: the radar station below as important target 1, the command building as important target 2, and the radar station above as important target 3. The coordinates of the three important targets are shown in Table 1. As shown in Figure 4, the important targets are established as the command building and the radar station, the farthest point of the island and reef is selected as the coordinate point of the search area and as the search range of the UAV, and the boundary point of the UAV flight turning (blue) is further obtained.

Table 1. Three important target coordinates of Hongxiu Island.

Target coordinates	Radar station 1	Command post	Radar station 2
x	530	1500	970
y	570	600	450

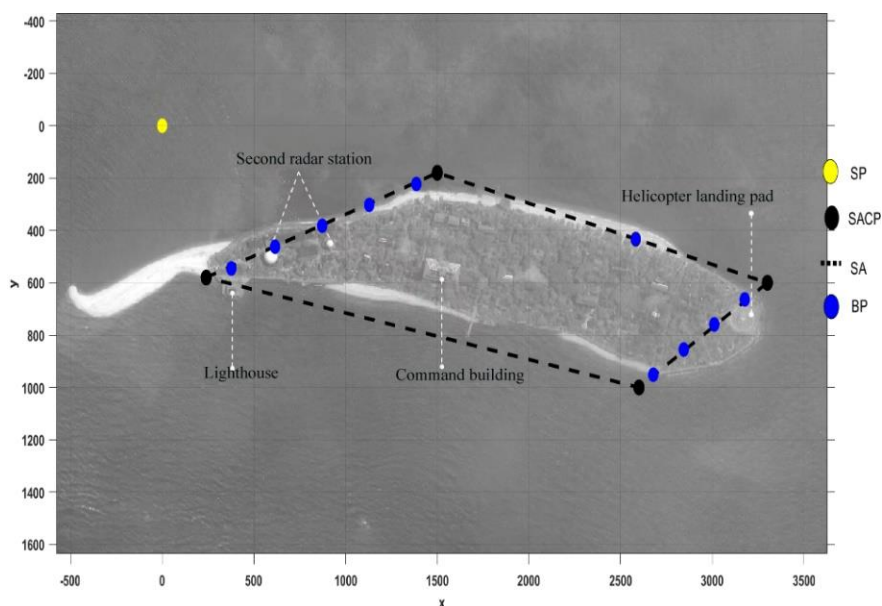


Figure 4. Search range map of Hongxiu Island (The abbreviations are described in Appendix A).

3.2. Multiple UAVs coverage path of Jinghong Island under priority of missile launcher

Considering the case of limited operators, one operator and two UAVs can be taken as an experiment to obtain the shortest coverage path of Jinghong Island, as shown in Figure 5. The starting point of the UAV can be located at the lower left of the figure (yellow coordinate point), the two UAVs can perform a parallel search coverage (routes are red and green straight lines), and the route back to the starting point can be dotted by a line. A total of 16 turning points can be used to complete the search coverage. Among the search process, the first UAV can fly through 8 turning points to preferentially search the missile launcher target. The second UAV can fly through eight steering points, mainly covering the range such as the site dock; the coordinates of the two UAVs are shown in Tables S1 and S2 of Appendix B.

The abbreviations are described in Appendix A. O-U1, O-U2: The steering point during the flight of the first and second UAV with the missile launcher preferential search, respectively. T-U1 L(RL), T-U2 L(RL): The line (return line) during the flight of the first and second UAV with the missile launcher preferential search, respectively. The red rectangular box represents the target.

Considering the case of relatively sufficient operators, two operators and three UAVs are taken as the second experiment to obtain the coverage path of Jinghong Island with the shortest time, as shown in Figure 6. The starting point of the UAV can be located at the lower left of the figure (yellow coordinate point), the three UAVs perform a parallel search coverage (the routes are red, green, and blue straight lines, respectively), and the routes returning to the starting point can be dotted by lines. Under the condition of a priority search for the missile launcher, a total of 16 turning points have been passed to complete the search coverage. Among the search process, the first UAV can fly through 4 turning points to complete the task of a target search and coverage area. The second UAV can fly through eight steering points, mainly covering the living area of the island and reef. The third UAV can fly through four steering points covering the site dock area, and the coordinates of the three UAVs are shown in the Tables S3–S5 of Appendix B.

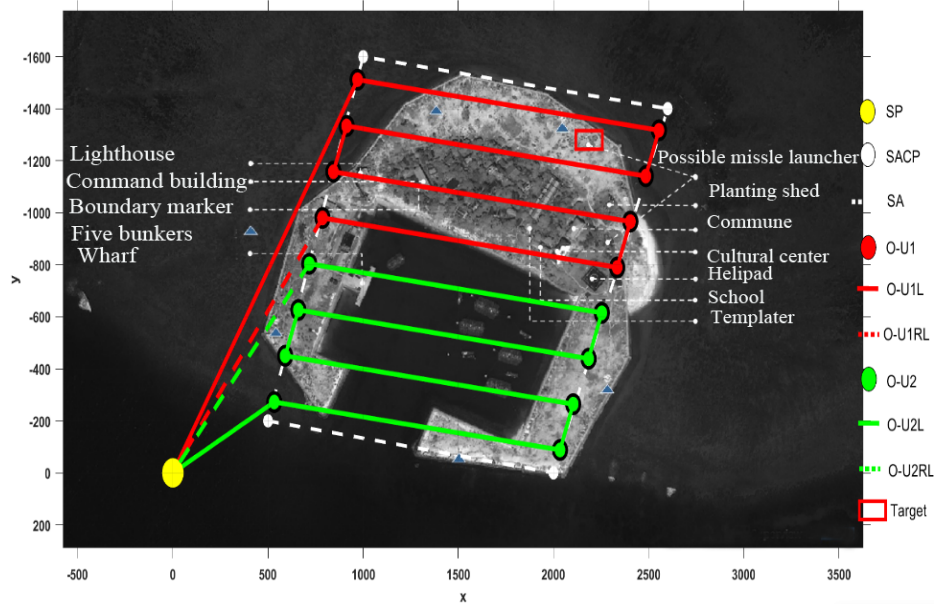


Figure 5. Coverage of Jinghong Island with two UAVs.

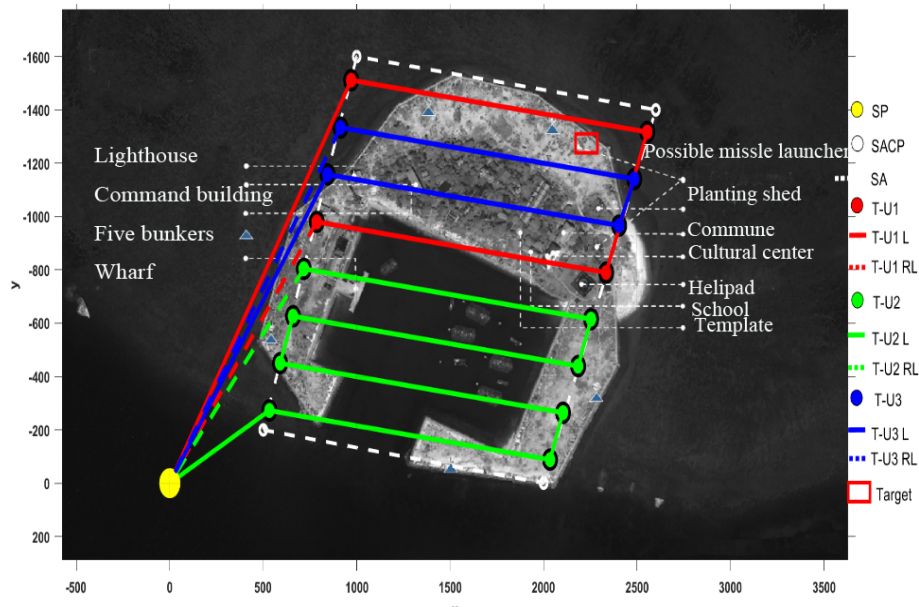


Figure 6. Coverage of Jinghong Island with two operators and three UAVs.

The abbreviations are described in Appendix A. T-U1, T-U2, T-U3: The steering point during the flight of the first, second, and third UAV with a missile launcher preferential search, respectively. T-U1 L (RL), T-U2 L (RL), T-U3 L (RL): The line (return line) during the flight of the first, second, and third UAV with a missile launcher preferential search, respectively. The red rectangular box represents the target.

3.3. Multiple UAVs coverage path of Hongxiu Island under priority of three High-value goals

Considering the case of limited operators, one operator and two UAVs are taken as the first

experiment to obtain the shortest coverage path of Hongxiu Island, as shown in Figure 7. The starting point of the UAV can be located at the top left of the figure (yellow coordinate point), the two UAVs perform a parallel search coverage (routes are red and green straight lines, respectively), and the routes returning to the starting point can be dotted by lines. A total of 10 turning points are used to complete the search coverage, among which, the first UAV can fly through 4 turning points. The second UAV can fly through six steering points, and the coordinates of two UAVs are shown in Tables S6 and S7 of Appendix B. The time required to complete the search coverage can be taken by 16.6627 minutes.

Considering the case of relatively sufficient operators, two operators and three UAVs are taken as the second experiment to obtain the coverage path of Hongxiu Island with the shortest time, as shown in Figure 8. The starting point of the UAV can be located at the top left of the figure (yellow coordinate point), the three UAVs perform a parallel search coverage (the routes are red, green, and blue straight lines, respectively), and the routes returning to the starting point can be dotted by lines. A total of 10 turning points are used to complete the search coverage. Among the search process, the first UAV can fly through 4 turning points. The second UAV can fly through four steering points. The third UAV can fly through 2 steering points, and the coordinates of three UAVs are shown in Tables S8–S10 of Appendix B. The time completed the search coverage can be taken by 10.9830 minutes.

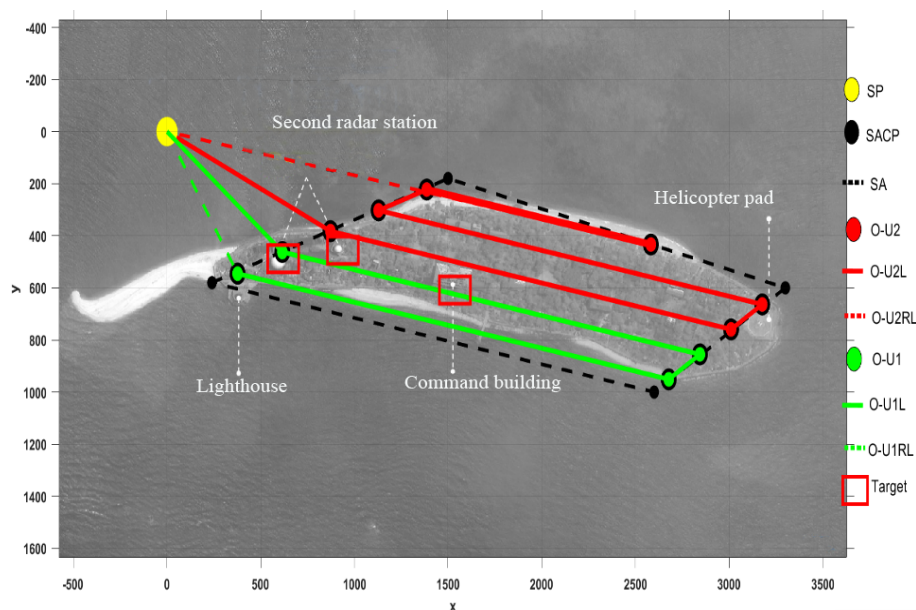


Figure 7. Coverage map of important targets in Hongxiu Island.

The abbreviations are described in Appendix A. O-U1, O-U2: The steering point during the flight of the first and second UAV with a three-target preferential search, respectively. T-U1 L (RL), T-U2 L (RL): The line (return line) during the flight of the first and second UAV with a three-target preferential search, respectively. The red rectangular box represents target.

The abbreviations are described in Appendix A. T-U1, T-U2, T-U3: The steering point during the flight of the first, second, and third UAV with a three-target preferential search, respectively. T-U1 L (RL), T-U2 L(RL), T-U3 L(RL): The line (return line) during the flight of the first, second, and third UAV with a three-target preferential search, respectively. The red rectangular box represents the target.

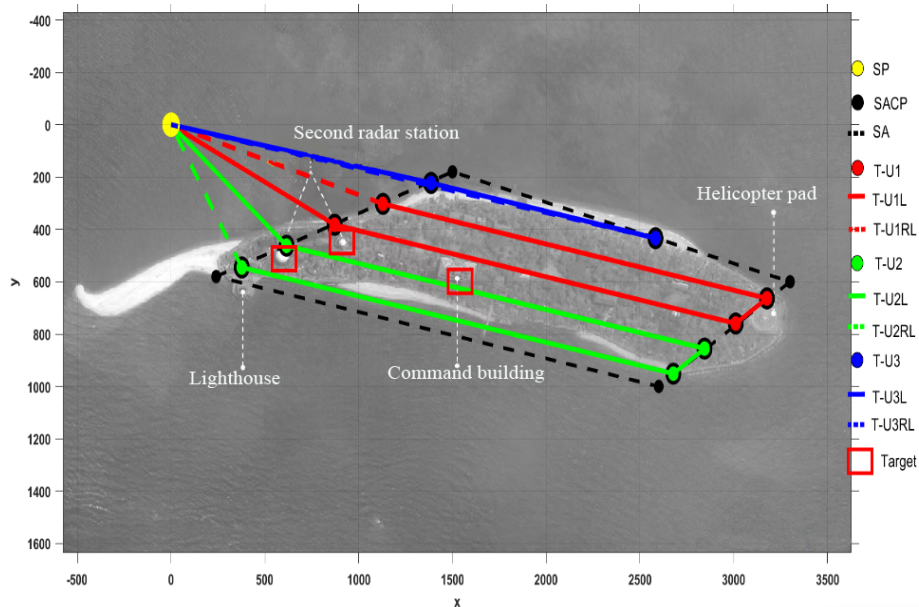


Figure 8. Coverage path of Hongxiu Island with multiple operators.

3.4. Comparison of search coverage way and time on four islands

3.4.1. Multi-UAVs path coverage of Jinghong Island under uniform decomposition

Other coverage paths of Jinghong Island can be used to verify the scheme that the first and second UAVs search three rows each and the third UAV searches two rows for an approximate uniform coverage; therefore, the size of the area to be covered by each UAV can be uniform of a decomposition, as shown in Figure 9. This scheme can take 13.7613 minutes to complete the search coverage.

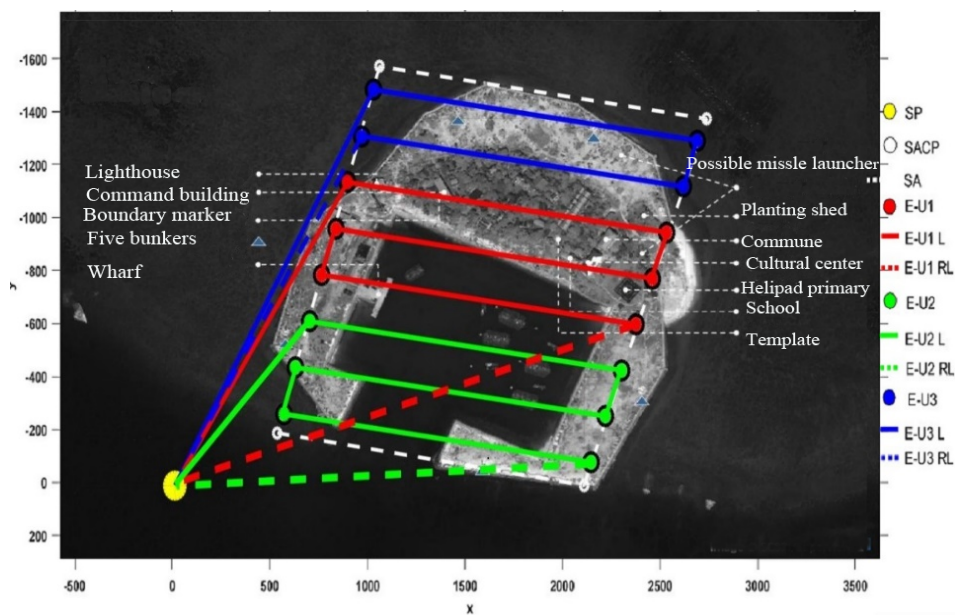


Figure 9. Coverage path of Jinghong Island under uniform segmentation.

The abbreviations are described in Appendix A. E-U1, E-U2, E-U3: The steering point during the flight of the first, second, and third UAV with areas of a similar size, respectively. E-U1 L (RL), E-U2 L (RL), E-U3 L (RL): The line (return line) during the flight of the first, second, and third UAV with areas of a similar size search, respectively.

3.4.2. Hongxiu Island coverage scheme under single operator

In order to better compare the applicability of the proposed method, consider the case of limited operators, assume that one operator and two UAVs are taken as an example, and the coverage path with the shortest time can be obtained, as shown in Figure 10. The starting point of the UAV can be located at the top left of the figure (yellow point), the 2 UAVs can perform a parallel search coverage (routes are red and green straight lines, respectively), and routes returning to the starting point can be dotted by lines. A total of 10 turning points have been passed, and the time completed the search coverage can be taken by 14.6627 minutes.

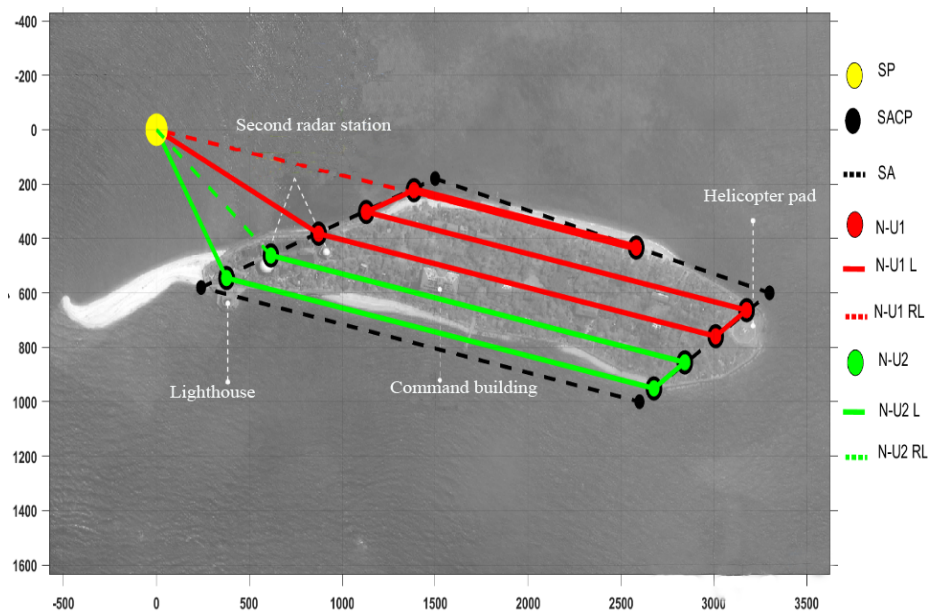


Figure 10. Coverage map of Hongxiu Island with one operator.

N-U1, N-U2: The steering point during the flight of the first and second UAV without a target priority, respectively. N-U1 L (LR), N-U2 L(LR): The line (return line) during the flight of the first and second UAV without a target priority, respectively.

3.4.3. Comparison of search coverage time on four islands

As shown in Figure 11, the total flight time of the UAV search can be compared under three types of search operations on Jinghong Island, including single operator double UAVs (O-U1, O-U2), double operator three UAVs (T-U1, T-U2, T-U3), and a uniform coverage under three UAVs (E-U1, E-U2, E-U3). Increasing the number of operators and UAVs can indeed reduce the search time of the whole area. Along with the statistics about the heights of the bars under the three classes of UAV operation settings, the time difference of each UAV search based on the target priority can be relatively small, which can further illustrate the adaptability of the search region segmentation and the rationality of UAV turning-

point matching. The coverage scheme with two operators and three UAVs can take 13.1539 minutes, which is 0.6074 minutes faster than the approximate uniform coverage scheme. Compared with the search process of a single operator, the path coverage time with a multiple-target priority is 2.088 minutes faster, which can prove that the proposed method can have an improved search efficiency. As described in Figure 11, the total flight time of the UAV search can be compared under three types of search methods on Hongxiu Island, alongside the statistics about the total flight time of the UAVs, including the pure coverage with single operator and double UAVs (N-U1, N-U2), the three-target preferential search coverage with single operator and double UAVs (O-U1, O-U2), and the three-target preferential search coverage with double operator and three UAVs (T-U1, T-U2, T-U3). A multiple-target priority search can increase the total coverage time of the area, and the shortest search time by different UAVs greatly varies. In the case of ensuring a multi-target priority, the coverage time of three UAVs has been 5.6797 minutes faster than that of the scheme with two UAVs. In the third type of search mode, it can be clearly seen that the search time difference of each UAV is relatively small, which determines that the overall search cost can be reduced with a high utilization rate and with a higher efficiency. Increasing the number of UAVs can quickly reduce the overall coverage time, and illustrate the adaptability of the region search modeling and the rationality of UAV turning-point matching.

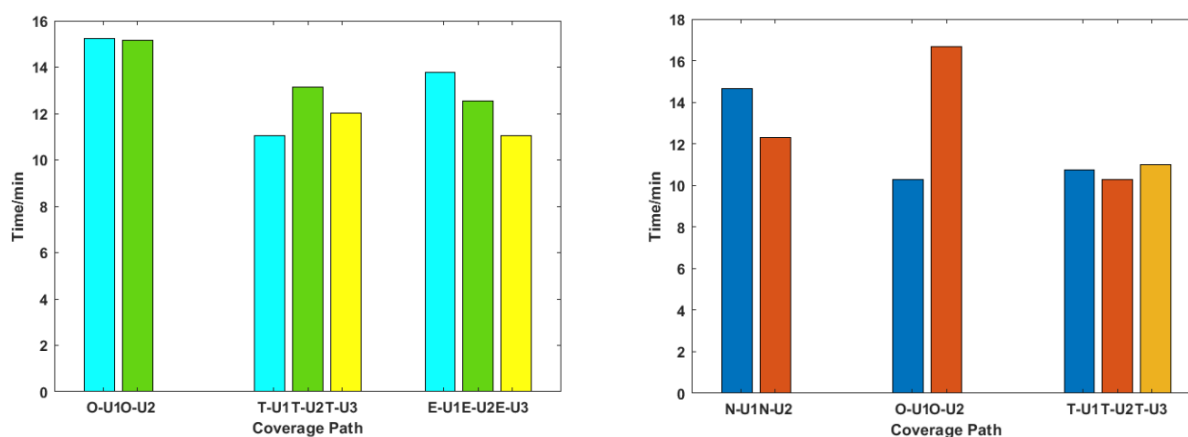


Figure 11. Comparison of search coverage time with different search ways on Jinghong Island (up) and on Hongxiu Island (down).

In order to better detect the performance of the proposed method, we have compared with two popular methods (ACO and GD algorithm) [15,16] about the coverage time of more scenarios (Jinghong Island, Hongxiu Island, Dunqian Shazhou, and Middle Reef) with different numbers of UAVs (the result of ACO method is shown in Figures S1–S4). As shown in Figure 12, the experimental results show that the proposed method has an improved effect in the task time of the reef coverage in four islands with a higher coverage efficiency (CE). With an increase of the number of UAVs, the coverage efficiency of the proposed method increases the most. Among them, the search coverage efficiency of the two UAVs for the four islands and reefs is 28–38% higher than that of the ACO method, and the search coverage efficiency of the three UAVs is 40% higher than that of the ACO method, among which Hongxiu Island has the highest search efficiency, exceeding 55%. Furthermore, the search coverage efficiency of the three UAVs is higher than the coverage time of the GD method. With the increase in the number of drones, the coverage efficiency of the proposed method rapidly increases. It is worth noting that in the double UAV search and coverage of Hongzhou Island, the GD method performs better, which may be related to the priority search of the three targets of the island.

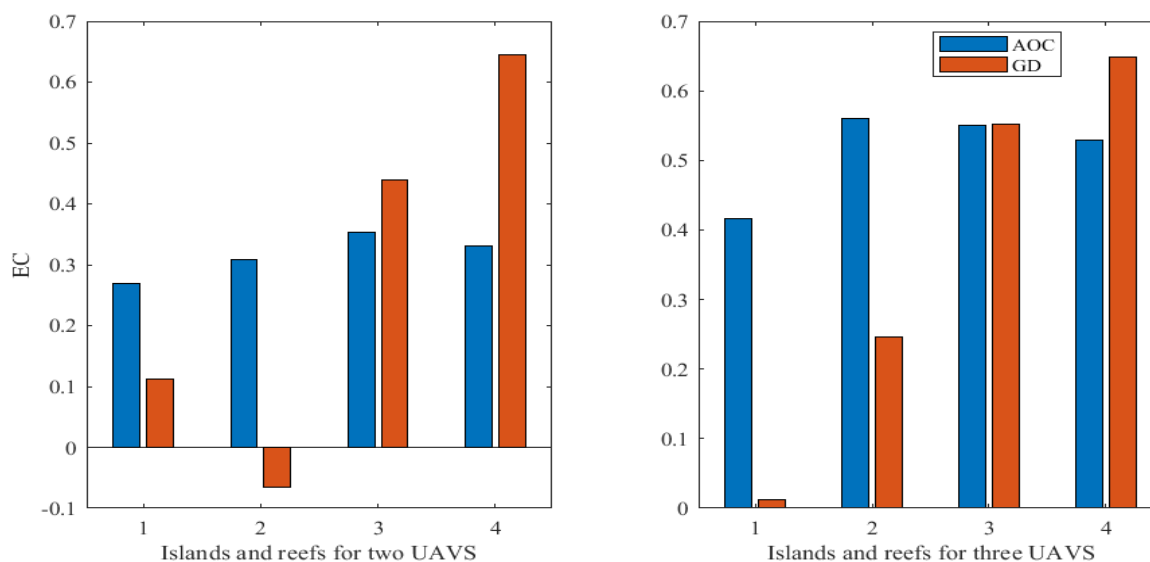


Figure 12. Comparison of coverage efficiency (CE) with ACO and GD method.

4. Conclusions

Aiming at the actual situation that the number of operators is less than the number of UAVs in the process of performing specific tasks, a multi-UAV coverage model was proposed based on a multi-objective priority search under a domain decomposition strategy, and the path coverage strategy with an optimal time was studied. By setting different numbers of operators and UAVs, the priority path coverage scheme of important targets in four islands was realized to have a higher efficiency under the model, which better illustrated the adaptability and reliability of the proposed method. Compared with a uniform area search and non-target search, the superiority and rationality of the proposed method was proven, which provided a reference for the real search coverage task. In the future, we will study how to make coping strategies for interference at any time.

Use of AI tools declaration

The authors declare they have not used Artificial Intelligence (AI) tools in the creation of this article.

Conflict of interest

The authors declare there is no conflict of interest.

References

1. Y. Li, W. Han, Y. Wang, Deep reinforcement learning with application to air confrontation intelligent decision-making of manned/unmanned aerial vehicle cooperative system, *IEEE Access*, **8** (2020), 67887–67898. <https://doi.org/10.1109/ACCESS.2020.2985576>
2. P. Radoglou-Grammatikis, P. Sarigiannidis, T. Lagkas, L. Moscholios, A compilation of UAV applications for precision agriculture, *Comput. Netw.*, **172** (2020), 1389–1286. <https://doi.org/doi:10.1016/j.comnet.2020.107148>

3. M. Pavone, E. Frazzoli, Decentralized policies for geometric pattern formation, in *2007 American Control Conference (ACC)*, (2007), 3949–3954. <https://doi.org/10.1109/ACC.2007.4283108>
4. M. Yao, X. Feng, P. Li, Y. Li, Z. Peng, Z. Lu, Object-level complete coverage path planning for excavators in earthwork construction, *Sci. Rep.*, **13** (2023), 12818. <https://doi.org/10.1038/s41598-023-40038-3>
5. J. Chen, F. Ling, Y. Zhang, T. You, Y. Liu, X. Du, Coverage path planning of heterogeneous unmanned aerial vehicles based on ant colony system, *Swarm Evol. Comput.*, **69** (2021), 101005. <https://doi.org/10.1016/j.swevo.2021.101005>
6. S. Aggarwal, N. Kumar, Path planning techniques for unmanned aerial vehicles: A review, solutions, and challenges, *Comput. Commun.*, **149** (2020), 270–299. <https://doi.org/10.1016/j.comcom.2019.10.014>
7. J. Chen, P. Han, Y. Zhan, T. You, P. Zheng, Scheduling energy consumption-constrained workflows in heterogeneous multi-processor embedded systems, *J. Syst. Architect.*, **142** (2023), 102938. <https://doi.org/10.1016/j.sysarc.2023.102938>
8. L. Yan, C. Hai, J. Meng, X. Wang, Coverage path planning for UAVs based on enhanced exact cellular decomposition method, *Mechatronics*, **21** (2011), 876–885. <https://doi.org/10.1016/j.mechatronics.2010.10.009>
9. R. S. Nilsson, K. Zhou, Method and bench-marking framework for coverage path planning in arable farming, *Biosyst. Eng.*, **198** (2020), 248–265. <https://doi.org/10.1016/j.biosystemseng.2020.08.007>
10. S. Ivić, A. Andrejčuk, S. Družeta, Autonomous control for multi-agent non-uniform spraying, *Appl. Soft Comput.*, **80** (2019), 742–760. <https://doi.org/10.1016/j.asoc.2019.05.001>
11. A. Bouras, Y. Bouzid, M. Guiatn, Areas division and multiple UAV coverage path planning for gas distribution map, in *19th International Multi-Conf. Systems (IMCS)*, (2022), 1554–1560. <https://doi.org/10.1109/SSD54932.2022.9955697>
12. Y. Choi, Y. Choi, S. I. Briceno, D. N. Mavris, Energy-constrained multi-UAV coverage path planning for an aerial imagery mission using column generation, *J. Intell. Robot. Syst.*, **97** (2020), 125–139. <https://doi.org/10.1007/s10846-019-01010-4>
13. Y. Jin, Pareto-based multi-objective machine learning, in *7th International Conference on Hybrid Intelligent Systems (ICHIS)*, (2007), 2. <https://doi.org/10.1109/HIS.2007.73>
14. G. Avellar, G. Pereira, L. Pimenta, P. Iscold, Multi-UAV routing for area coverage and remote sensing with minimum time, *Sensors*, **15** (2015), 27783–27803. <https://doi.org/10.3390/s151127783>
15. Y. Jia, S. Zhou, Q. Zeng, C. Li, D. Chen, K. Zhang, et al., The UAV path coverage algorithm based on the greedy strategy and Ant Colony optimization, *Electronics*, **11** (2022), 2667. <https://doi.org/10.3390/electronics11172667>
16. S. Cho, J. Park, H. Park, S. Kim, Multi-UAV coverage path planning based on hexagonal grid decomposition in maritime search and rescue, *Mathematics*, **10** (2022), 83. <https://doi.org/10.3390/math10010083>
17. M. Popović, T. Vidal-Calleja, G. Hitz, I. Sa, R. Siegwart, J. Nieto, Multiresolution mapping and informative path planning for UAV-based terrain monitoring, in *2017 IEEE/RSJ International Conference Intelligent Robots and System (IIRCIRS)*, (2017), 1382–1388. <https://doi.org/10.1109/IROS.2017.8202317>

18. D. Chanchal, K. Pawan, An improved weighted sum-fuzzy Dijkstra's algorithm for shortest path problem, *Soft Comput.*, **26** (2022), 3217–3226. <https://doi.org/10.1007/s00500-022-06871-w>
19. H. Wang, J. Zhou, G. Zheng, Y. Liang, HAS: Hierarchical A-Star algorithm for big map navigation in special areas, in *2014 5th International Conference Digital Home (ICDH)*, (2014), 222–225. <https://doi.org/10.1109/ICDH.2014.49>
20. G. Hu, J. Zhong, G. Wei, SaCHBA_PDN: modified honey badger algorithm with multi-strategy for UAV path planning, *Expert Syst. Appl.*, **223** (2023), 119941. <https://doi.org/10.1016/j.eswa.2023.119941>
21. M. Yuan, T. Zhou, M. Chen, Improved lazy theta algorithm based on octree map for path planning of UAV, *Def. Technol.*, **2** (2023), 8–18. <https://doi.org/10.1016/j.dt.2022.01.006>
22. J. A. GoncaAlves, R. Henriques, UAV photogrammetry for topographic monitoring of coastal areas, *Isprs J. Photogramm.*, **104** (2015), 101–111. <https://doi.org/10.1016/j.isprsjprs.2015.02.009>
23. A. Batyra, M. D. Vroey, From one to many islands: the emergence of search and matching models, *B. Econ. Res.*, **64** (2011), 393–414. <https://doi.org/10.1111/j.1467-8586.2010.00389.x>
24. D. G. Reina, H. Tawfik, S. L. Toral, Multi-subpopulation evolutionary algorithms for coverage deployment of UAV-networks, *Ad Hoc Netw.*, **68** (2018), 16–32. <https://doi.org/10.1016/j.adhoc.2017.09.005>
25. H. Song, J. Yu, J. Qiu, Z. Sun, K. Lang, Q. Luo, et al., Multi-UAV disaster environment coverage planning with limited-endurance, in *2022 International Conference Robotics and Automation (ICRA)*, (2022), 10760–10766. <https://doi.org/10.1109/ICRA46639.2022.9812201>
26. A. B. Bugnot, M. Mayer-Pinto, L. Airoidi, E. C. Heery, E. L. Johnston, L. P. Critchley, et al., Current and projected global extent of marine built structures, *Nat. Sustain.*, **4** (2021), 33–41. <https://doi.org/10.1038/s41893-020-00595-1>
27. S. Xiao, X. Tan, J. Wang, A simulated annealing algorithm and grid map-based UAV coverage path planning method for 3D reconstruction, *Electronics*, **10** (2021), 853. <https://doi.org/10.3390/electronics10070853>
28. J. Chen, T. Li, Y. Zhang, T. You, Y. Lu, P. Tiwari, et al., Global-and-local attention-based reinforcement learning for cooperative behaviour control of Multiple UAVs, *IEEE Trans. Veh. Technol.*, **73** (2023), 1–13. <https://doi.org/10.1109/TVT.2023.3327571L>
29. L. Lin, M. A. Goodrich, Hierarchical heuristic search using a gaussian mixture model for UAV coverage planning, *IEEE Trans. Cybern.*, **44** (2014), 2532–2544. <https://doi.org/10.1109/TCYB.2014.2309898>
30. S. Pulit, L. T. Ene, T. Gobakken, E. Naeset, Use of partial-coverage UAV data in sampling for large scale forest inventories, *Remote Sens. Environ.*, **194** (2017), 115–126. <https://doi.org/10.1016/j.rse.2017.03.019>
31. H. Wu, X. Tao, N. Zhang, X. Shen, Cooperative UAV cluster-assisted terrestrial cellular networks for ubiquitous coverage, *IEEE J. Sel. Areas Comm.*, **36** (2018), 2045–2058. <https://doi.org/10.1109/JSAC.2018.2864418>

Appendix A

SA represents Search area; SP represents Start position; SACP represents Search area coordinate points; BP represents Boundary point; OR represents Overlay Rows.

Appendix B

Table S1. The eight steering points during the flight of first UAV with missile launcher preferential search of Jinghong Island.

Target coordinates	1	2	3	4	5	6	7	8
x	530	1500	970	912.95	843.71	2403.89	2334.65	786.20
y	570	600	450	-1333.71	-1157.56	-965.99	-789.84	-979.97

Table S2. The eight steering points during the flight of second UAV with missile launcher preferential of Jinghong Island.

Target coordinates	1	2	3	4	5	6	7	8
x	532.70	2034.25	2103.49	590.22	659.45	2184.45	2253.69	716.96
y	-272.49	-88.12	-264.27	-450.08	-626.23	-438.98	-615.13	-803.82

Table S3. The four steering points during the flight of the first UAV with missile launcher preferential search of Jinghong Island.

Target coordinates	1	2	3	4
x	970.46	2554.09	2484.85	912.95
y	-1511.30	-1316.86	-1140.71	-1333.71

Table S4. The eight steering points during the flight of the second UAV with missile launcher preferential search of Jinghong Island.

Target coordinates	1	2	3	4	5	6	7	8
x	532.70	2034.25	2103.49	590.22	659.45	2184.45	2253.69	716.96
y	-272.49	-88.12	-264.27	-450.08	-626.23	-438.98	-615.13	-803.82

Table S5. The four steering points during the flight of third UAV with missile launcher preferential search of Jinghong Island.

Target coordinates	1	2	3	4
x	843.71	2403.89	2334.65	786.20
y	-1157.56	-965.99	-789.84	-979.97

Table S6. The four steering points during the flight of the first UAV under priority of three High-value goals of Hongxiu Island.

Target coordinates	1	2	3	4
x	615.55	2844.19	2677.89	376.81
y	462.28	855.24	951.13	545.39

Table S7. The six steering points during the flight of the second UAV under priority of three High-value goals of Hongxiu Island.

Target coordinates	1	2	3	4	5	6
x	872.39	3010.48	3176.77	1129.23	1386.07	2582.44
y	382.36	759.36	663.47	302.44	222.52	433.47

Table S8. The four steering points during the flight of the first UAV under priority of three High-value goals of Hongxiu Island.

Target coordinates	1	2	3	4
x	872.39	3010.48	3176.77	1129.23
y	382.36	759.36	663.47	302.44

Table S9. The four steering points during the flight of second UAV under priority of three High-value goals of Hongxiu Island.

Target coordinates	1	2	3	4
x	615.55	2844.19	2677.90	376.81
y	462.28	855.24	951.13	545.39

Table S10. The two steering points during the flight of the third UAV under priority of three High-value goals of Hongxiu Island.

Target coordinates	1	2
x	1386.07	2582.44
y	222.52	433.47

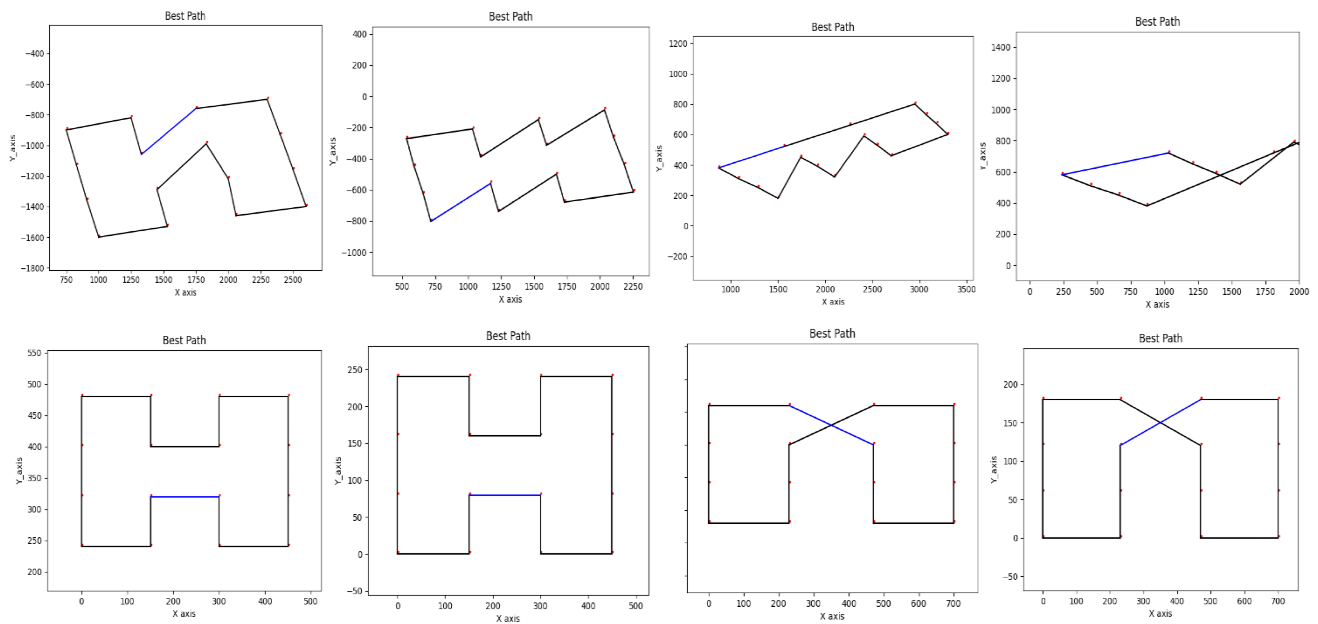


Figure S1. The path coverage route of the two UAVs for the four islands and reefs under the ACO method.

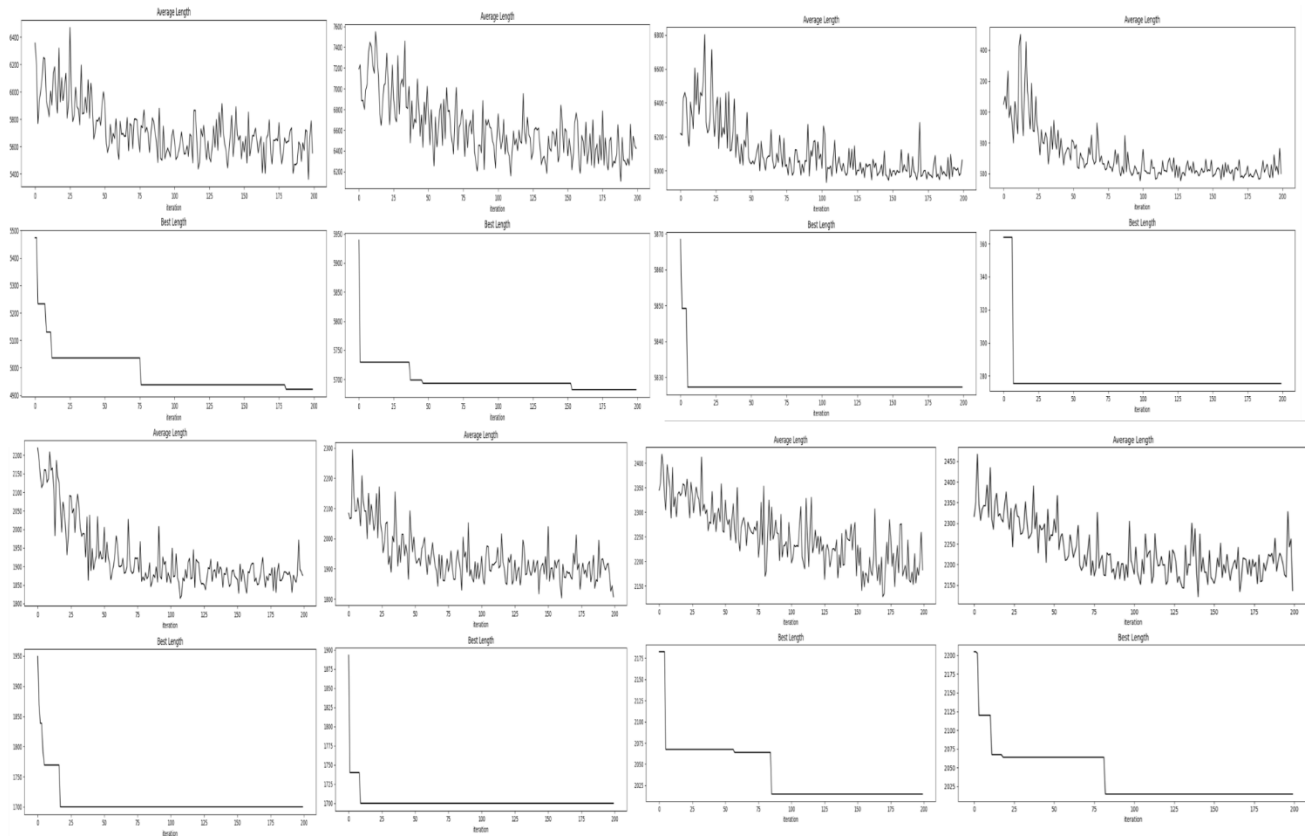


Figure S2. The average and total distance of the path coverage route of the two UAVs for the four islands and reefs under the ACO method.

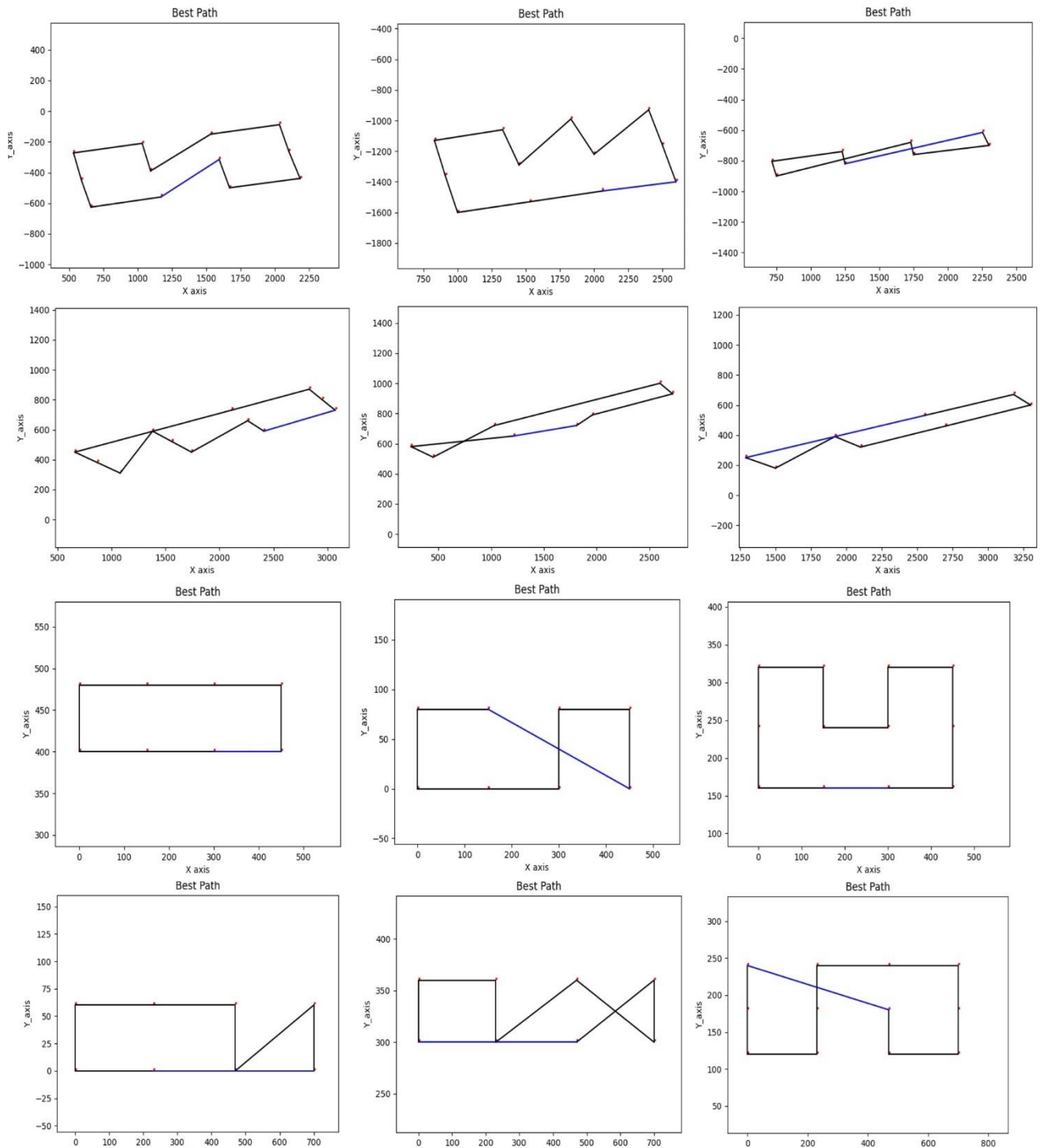


Figure S3. The path coverage route of the three UAVs for the four islands and reefs under the ACO method.

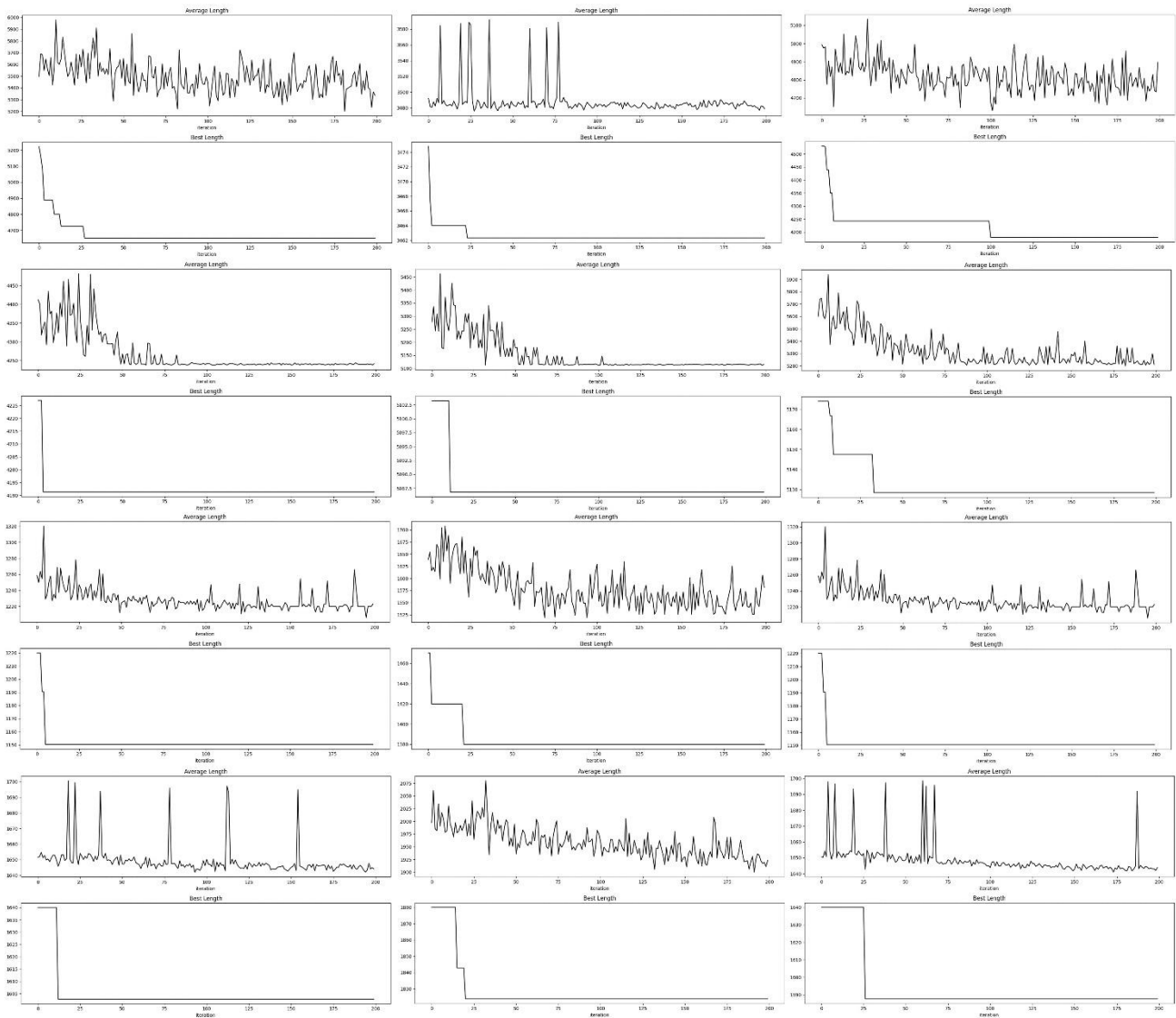


Figure S4. The average and total distance of the path coverage route of the two UAVs for the four islands and reefs under the ACO method.



©2024 the Author(s), licensee AIMS Press. This is an open access article distributed under the terms of the Creative Commons Attribution License (<http://creativecommons.org/licenses/by/4.0>)